JOURNAL OF MATERIALS SCIENCE 28 (1993) 1874–1878

Electron microscopic study of fine particles of beryllium

P. J. HERLEY
Department of Materials Science and Engineering, State University of New York, Stony Brook, NY 11794, USA

W. JONES
Department of Chemistry, University of Cambridge, Lensfield Road, Cambridge CB2 1EW, UK

It is demonstrated that nanometre-sized particles of beryllium may be readily generated *in situ* by the electron-beam induced decomposition of BeH_2 within a transmission electron microscope. The particles, to a first approximation, are distributed around two well-defined sizes, each size with its own distinct morphology: the first are hexagonal plates (approximately 1.5 μm) and the second are slightly polygonized spheres of dimensions between 1 and 5 nm. The morphological form of these particles is presented and discussed as well as the electron energy loss spectrum and some high-resolution lattice images. The results are compared with those obtained for other metal hydrides.

1. Introduction

We have previously examined, using transmission electron microscopy (TEM), a variety of lightweight metal hydrides including $NaAlH_4$ [1, 2], AlH_3 [3], MgH_2 [4], ScH_2 [5] and CuH [6, 7]. Our aim in these studies has been two-fold: firstly, to identify any additional (secondary) phases present in the hydrided material, and secondly, for the pristine solid material, to elucidate the nature of any crystal imperfections which may be present and to determine their role, if any, in the release (or uptake) of hydrogen gas. The studies were particularly essential from the viewpoint of understanding the role of defects in such solids given their potential use in the removal/uptake of hydrogen gas in hydrogen storage and transportation systems.

It soon emerged, however, that lightweight metal hydrides rapidly decompose as the direct result of their electron-beam sensitivity, with simultaneous hydrogen gas evolution. Notwithstanding this beam sensitivity, we were able to identify several types of crystalline defects including twins, stacking faults and grain boundaries, as well as the existence of secondary phases in a variety of hydrides [8, 9].

Few studies have been made to date of the morphology of fine particles of beryllium apart from that of work on beryllium smokes [10, 11], produced by burning beryllium metal in xenon vapour and in which micrometre-sized hexagonal platelets and polygonized spheres of h c p alpha-beryllium were produced. These were entirely of micrometre dimensions and no nanometre-sized particles were examined.

In the study reported here the morphology and microstructure of the particles which result from electron-beam induced hydride decomposition are examined. We show that BeH_2, like the previously studied hydrides, generates ultra-fine particles of beryllium metal when subjected to intense electron irradiation. High-resolution lattice images of the particles are reported, together with electron energy loss (EEL) spectra. The EEL data are compared with computed and measured values for other hydrides and their metallic decomposition products.

2. Experimental procedure

Beryllium hydride, BeH_2, is difficult to prepare, not obtainable directly from the combination of its elements and is sensitive to air. Very little is known about its physical and chemical properties. The full crystal structure has, however, been recently determined [12]. Material for our study was kindly supplied by Dr P. E. Barry, Tritium Technology Section, Lawrence Livermore Laboratory. The purity, as reported, was 94.3% BeH_2, 2.3% beryllium metal with a mixture of BeO, beryllium alkyls and beryllium alkoxides comprising the remaining 3.4%. Samples were stored in the dark under an atmosphere of helium.

Prior to investigation in the electron microscope the material was ground and then transferred to a holey-carbon specimen support grid using dry toluene, ether or iso-pentane solvents, in which the hydride is insoluble. X-ray dispersive analysis confirmed that there were no other major metallic impurities. TEM observations were made, at room temperature, using either a JEOL 200CX TEMSCAN or a Phillips CM12 microscope with a Gatan PEELS attachment.

3. Results and discussion

3.1. Nature of the beam-induced decomposition process

A micrograph of the pristine material with minimal

0022–2461

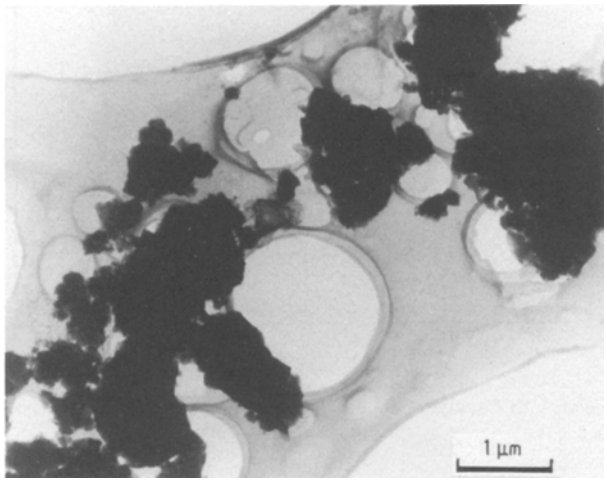

Figure 1 As-received material, supported on the holey carbon film, prior to beam decomposition. The material appears to consist of aggregates approximately 0.1–15 μm in size.

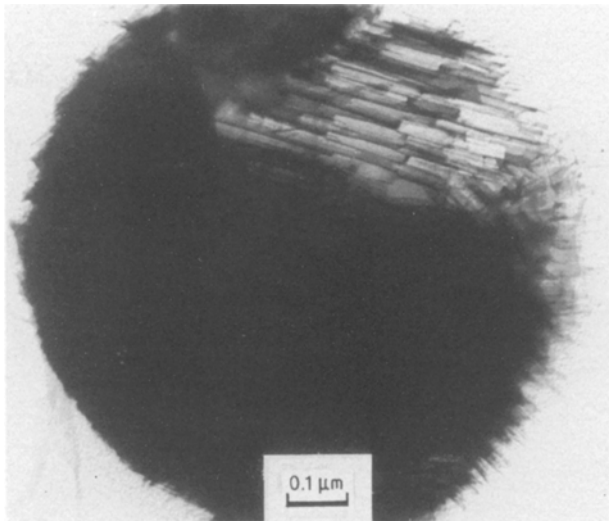

Figure 2 Residual bead generated after decomposition of the hydride. Subsequent beam irradiation does not result in remelting of the residue. The overall appearance is one of melting followed by recrystallization.

beam exposure is shown in Fig. 1. The overall crystallite sizes and their sensitivity to even minimal exposure excluded any defect analysis on the as-received material: similar comments have been made by previous workers [12]. This is not unexpected, as the reported (thermal) decomposition temperature is 125 °C. The sequence of events accompanying the beam-induced decomposition are as follows [7]. When continuously exposed to a condensed beam, the first noticeable effect is the rounding of crystal edges suggestive of melting. The onset of decomposition follows, detected by movement and shrinkage of the individual crystallites (Stage I). On further exposure to the beam, the melting process continues until eventually the material forms a molten bead (Stage II) which then decomposes and bubbles, depositing beryllium crystallites and a fine dust (Stage III) over the holey-carbon support. Deposition covers an area of the support a distance of 1–10 μm from the incident beam. Decomposition often continues briefly after the beam is removed, depositing additional fine particles over the areas originally covered by the initial deposition.

The residual bead, shown in Fig. 2, cannot be further decomposed upon re-irradiation, implying that the reactant hydride has been completely transformed to beryllium metal. The residual solidified bead appears at high magnification to consist of crystalline plates packed together.

The fine particles generated from the decomposition process (along with the larger hexagonal plates) are shown in Fig. 3. The nanometre-sized particles of beryllium appear as small dark regions on the background carbon. The larger well-defined hexagonal-shaped plates seen in this micrograph range from 0.5–5 μm in size.

3.2. Nature of the crystallites

Two distinct sizes of beryllium particles are observed, similar to those reported previously by Fukano and Nakao [10].

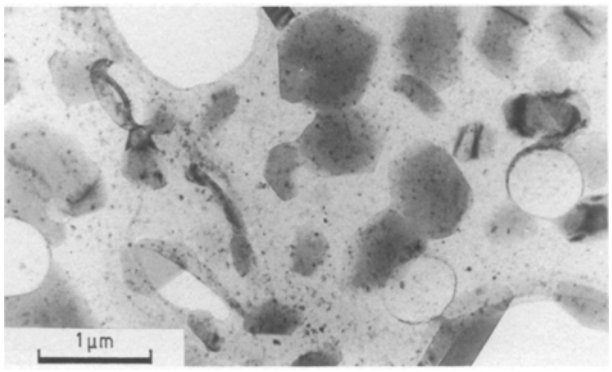

Figure 3 Low-magnification photograph of the beam-induced product resulting from irradiation of the molten beryllium hydride. There is a range of particle sizes as well as various particle morphologies.

3.2.1. Hexagonal platelets

The larger type are well-defined hexagonal platelets and are illustrated in Fig. 4a. The associated diffraction pattern indicates that they are single crystal in character, Fig. 4b. This would imply that the formation process is essentially one of homogeneous nucleation and growth. However, because of the presence of the product gas, heterogenous nucleation cannot be entirely ruled out. The presence of such well-defined particles would seem to indicate that the growth rate and the rate of nucleation are equally fast, thus enabling them to grow to their equilibrium shape in a short time. Most likely they represent first-order hexagonal plates, a common three-dimensional shape for crystal habits in h c p metals – more precisely a hexagonal bipyramid bounded by $\{10\bar{1}1\}$ and heavily truncated by $\{0001\}$ planes [11].

The platelets are very thin, approximately 100 nm, and are ideal for EEL plasmon spectra measurements. A typical EEL spectrum, taken in the diffraction mode on the centre spot for a beryllium platelet, is shown in Fig. 5. The plasmon peak position lies at 18.8 ± 4 eV

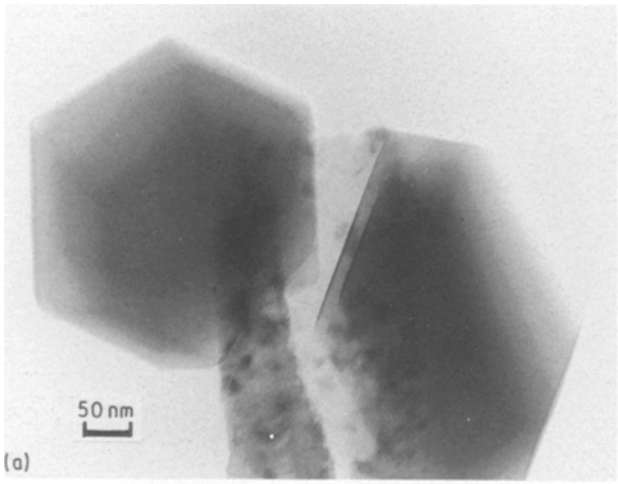

Figure 4 (a) High-magnification image of typical hexagonal platelets of α-beryllium, and (b) a diffraction pattern of a hexagonal platelet is also shown.

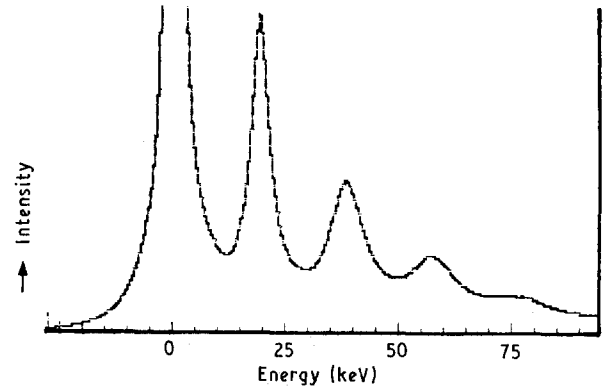

Figure 5 EEL spectrum for beryllium with loss peaks at multiples of 18.8 ± 4 eV.

TABLE I Observed, calculated and previously reported volume plasmon energies

System		Volume plasmon energy (eV)		
		Observed [16] (± 4 eV)	Reported [13]	Calculated [13,16]
Li from	LiH	7.2	7.08–7.12	8.0
	$LiAlH_4$	6.9–7.7		
Na from	NaH	5.6–5.9	5.6–5.72	6.0
	$NaAlH_4$	5.4		
	$NaBH_4$	5.4		
Mg from	MgH_2	10.0–13.0	10.0–10.5	11.0
	MgB_2	11.0		
Al from	AlH_3	15.3	14.92–15.03	16.0
Be from	BeH_2	18.8 (present work)	18.5–19.0	18.4

and compares well with other experimental values varying from 19.0–18.5 eV and a theoretical value of 18.4 eV [13]. Comparison of these data with the measured and theoretical values for all the hydrides measured to date, and the single-crystal particles generated from their beam sensitive precursors, is given in Table I.

Lattice imaging of these platelets produces images of very uniform thickness and contrast (Fig. 6). High-resolution images of this type prove that we are indeed looking along a direction close to ⟨0001⟩. It is also interesting that, in almost all cases, the particles do not overlap each other. This may be due to repulsive (electrostatic) surface charge effects between the particles.

3.2.2. Nanometre-sized particles

In general, faulting in these crystallites is not often observed. In the smaller polygonized-spherical particles, however, occasional faulted crystals are present, for example, see Fig. 7a. (The apparent absence of faulting in the ubiquitous hexagonal plates may be due to the faults lying parallel to the beam direction and thus not imaged.) Other habits are also encountered in the nanometre-size range; for example, truncated pyramids (Fig. 7b). These are similar to those observed for zinc, cadmium and other hcp metals [14].

3.2.3. Comparison with other hcp metals

The morphologies of magnesium particles generated from magnesium hydride are similar to those observed here for beryllium (Fig. 8a) [4]. Hexagonal platelets are readily formed and the particles have the same ⟨0001⟩ axis parallel to the beam. The crystallites are relatively thin, as evinced by the appearance of the bend extinction contours (Fig. 8b). The comparable size and shape of the magnesium and beryllium particles point to a similar growth process from their corresponding hydrides.

Overall, our observations are comparable to those made for dispersed particles generated from metallic smokes using evaporation techniques [14]. However, what is clear from our studies is that the use of

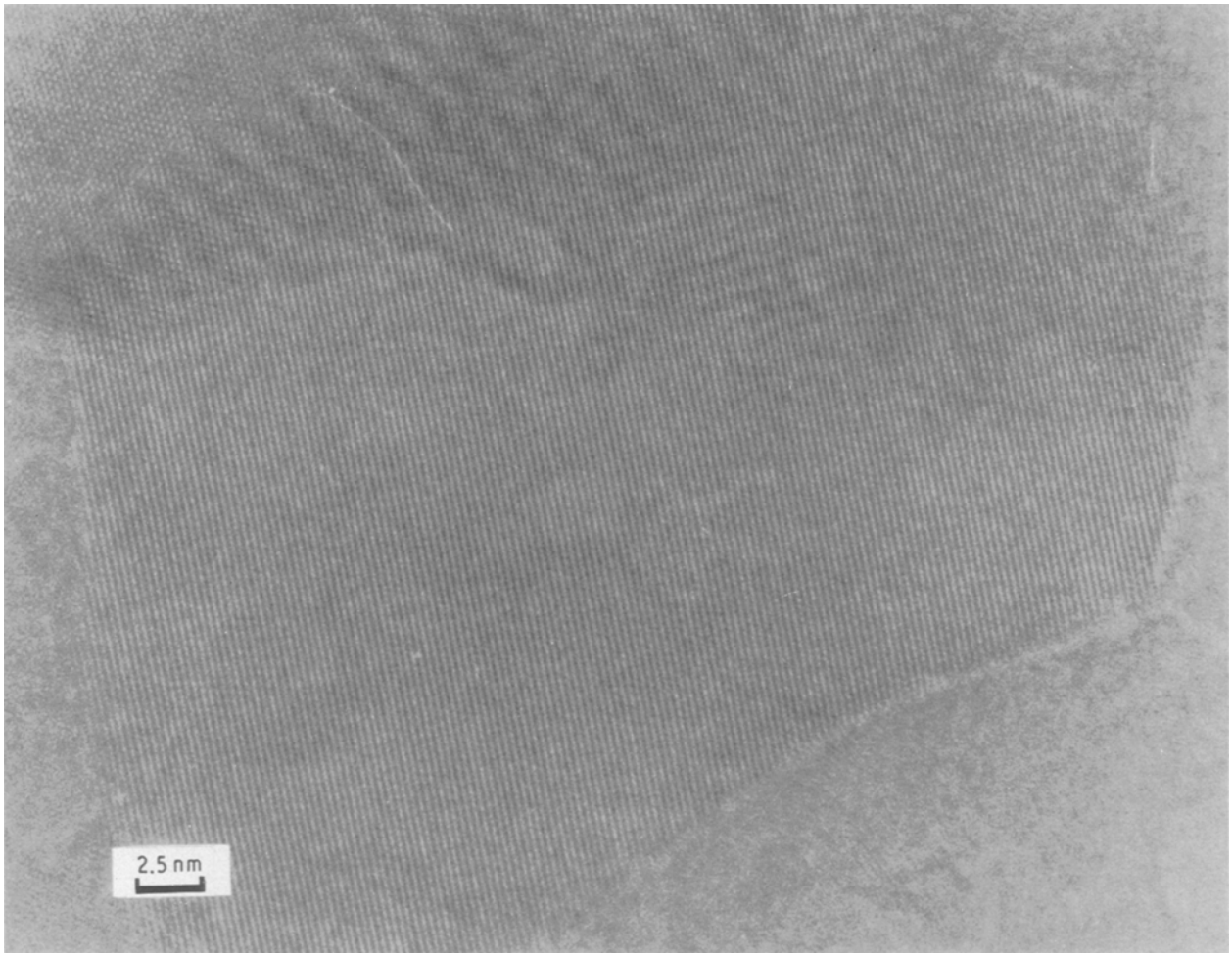

Figure 6 High-resolution image of beryllium microcrystals down ⟨0 0 0 1⟩ showing lattice fringes.

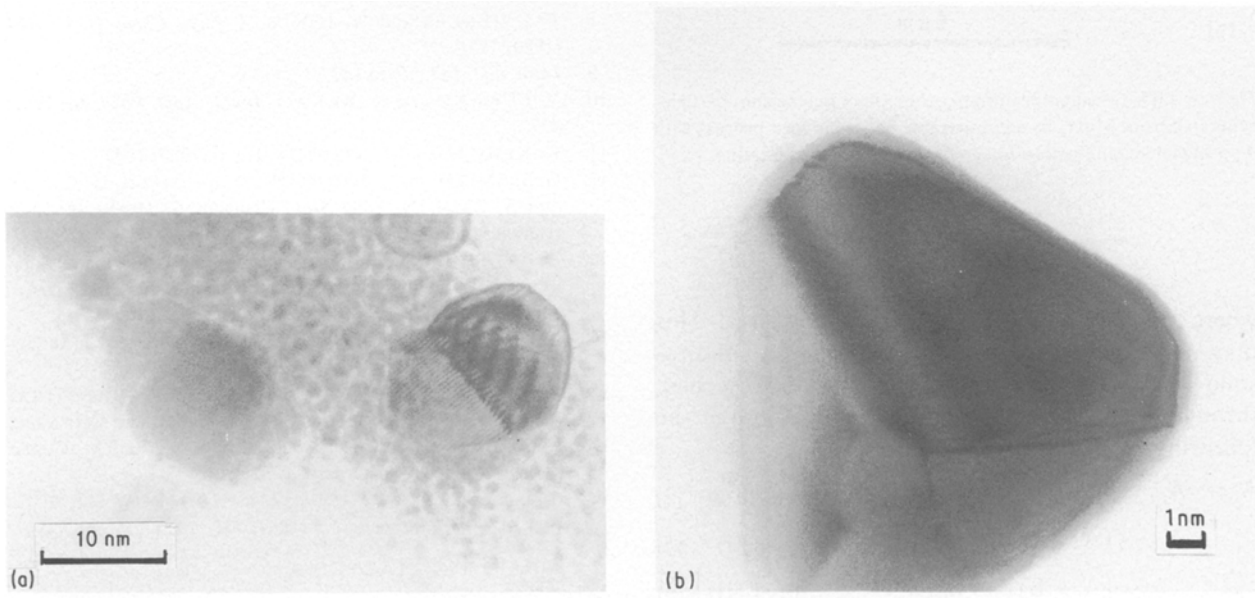

Figure 7 (a) Overlap of two non-facetted particles with the possible presence of a low-angle grain boundary, and (b) nanometre-size particle of beryllium approximately, 15 nm in size.

hydrides (and other beam-sensitive "binary" systems (e.g. azides) [7]) allows a facile and rapid procedure for the generation of dispersed ultra-fine particles. The particles can be generated as frequently as required, instantly and reproducibly.

3.2.4. Mechanism of particle formation

The overall electron-induced decomposition which takes place is

$$A_{(s)} \rightarrow B_{(s)} + H_{2(g)} \quad (1)$$

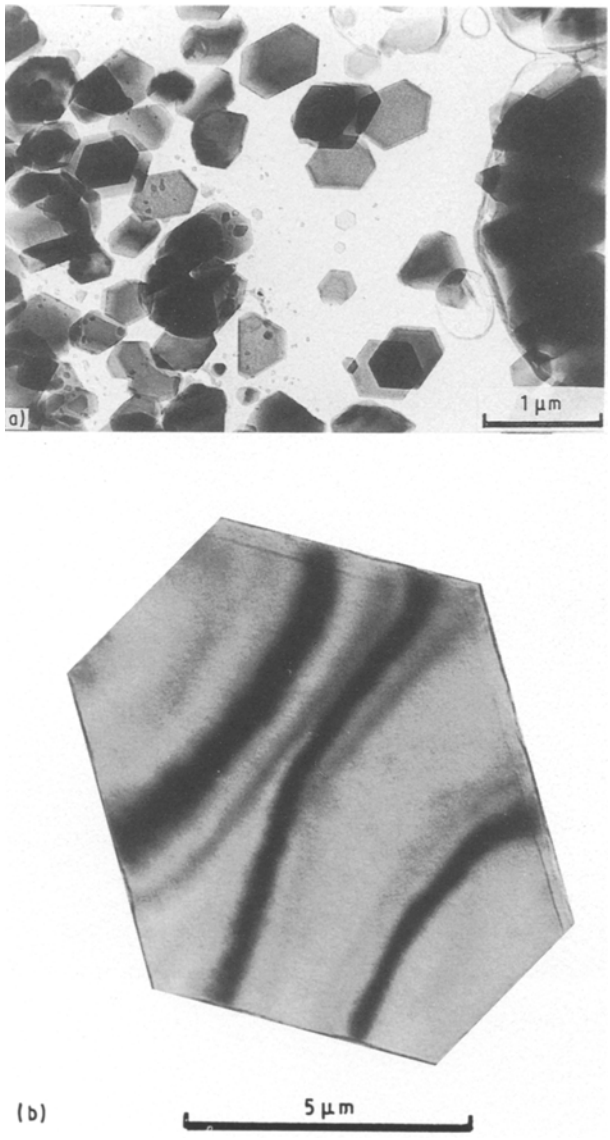

Figure 8 (a) Low-magnification photograph of magnesium particles generated from MgH_2 by a comparable beam-induced process with (b) a higher magnification image of an individual crystallite.

where A is the hydride and B the resulting metal. This may occur in at least two ways. First as a solid-to-solid transformation (without melting) or second, through a liquid intermediate, possibly through the following stages:

$$A_{(s)} \rightarrow A_{(l)} \quad \text{(Stage I)} \quad (2)$$

$$A_{(l)} \rightarrow [A + B]_{(l)} + H_{2(g)} \quad \text{(Stage II)} \quad (3)$$

$$[A + B]_{(l)} \rightarrow B_{(s)} + H_{2(g)} \quad \text{(Stage III)} \quad (4)$$

Stages II and III are rapid. A close experimental analogue of this process is electron hydrodynamic atomization [15]. Within the electron microscope the molten bead generates nanometre-sized crystallites as a result of the dispersion of the metal by the product gas. The nature of this hydride decomposition process is of interest, because our results indicate that the method provides a convenient and facile route to the preparation of highly dispersed nanometre-sized metallic particles of beryllium from beryllium hydride.

Acknowledgements

We thank Drs D. A. Jefferson and A. Kirkland for assistance with our electron microscopic studies. The financial support of the SERC, NSF (no. INT8911946), NATO through a collaborative research award (no. 890275) and VAL-ERO (contract DAJA45-90-C-0013) is appreciated.

References

1. P. J. HERLEY and W. JONES, *Mater. Lett.* **1** (1983) 131.
2. W. JONES, T. G. SPARROW, B. G. WILLIAMS and P. J. HERLEY, *ibid.* **2** (1984) 377.
3. P. J. HERLEY and W. JONES, *J. Mater. Sci. Lett.* **1** (1982) 163.
4. P. J. HERLEY, W. JONES and B. VIGEHOLM, *J. Appl. Phys.* **58** (1985) 292.
5. P. J. HERLEY and W. JONES, *Mater. Sci. Engng* **A114** (1989) L1.
6. P. J. HERLEY, W. JONES and G. R. MILLWARD, *J. Mater. Sci. Lett.* **8** (1989) 1013.
7. P. J. HERLEY, N. P. FITZSIMONS and W. JONES, in "Specimen Preparation for Transmission Electron Microscopy of Materials III", Materials Research Society, Vol. 254, edited by R. Anderson, J. Bravman and B. Tracy (1992) p. 223. Materials Research Society, Pittsburgh, Pennsylvania.
8. P. J. HERLEY and W. JONES, *Z. Phys. Chem. N. F* . **164** (1989) 1151.
9. *Idem, ibid.* **147** (1986) 147.
10. Y. FUKANO and K. NAKAO, *Jpn J. Appl. Phys.* **20** (1981) 477.
11. K. KIMOTO and I. NISHIDA *ibid.* **6** (1967) 1047.
12. G. S. SMITH, Q. C. JOHNSON, D. K. SMITH, D. E. COX and A. ZALKIN, *Solid State Commun.* **67** (1988) 491, and references therein.
13. H. RAETHER, "Excitation of Plasmons and Interband Transitions by Electrons", Springer Tracts in Modern Physics, Vol. 88 (Springer-Verlag, Berlin, 1980) p. 50.
14. R. UYEDA, in "Morphology of Crystals", edited by I. Sunagawa (Terra Scientific, Tokyo, 1987) Part B, Ch. 6.
15. J. PEREL, J. F. MAHONEY, S. TAYLOR, Z. SHANFIELD and C. LEVI, in "Rapid Solidified Amorphous and Crystalline Alloys", edited by B. H. Kear, B. C. Giessen and M. Cohen (North Holland, Amsterdam, 1982) p. 131.
16. P. J. HERLEY, W. JONES, T. G. SPARROW and B. G. WILLIAMS, *Mater. Lett.* **5** (1987) 333.

Received 15 June
and accepted 9 October 1992